Am J Physiol Heart Circ Physiol 291: H804–H812, 2006.
First published March 24, 2006; doi:10.1152/ajpheart.01262.2005.

Postnatal alterations in elastic fiber organization precede resistance artery narrowing in SHR

José M. González,[1] Ana M. Briones,[2] Beatriz Somoza,[1] Craig J. Daly,[3] Elisabet Vila,[2] Barry Starcher,[4] John C. McGrath,[3] M. Carmen González,[1] and Silvia M. Arribas[1]

[1]*Universidad Autónoma de Madrid, Madrid, Spain;* [2]*Universitat Autònoma de Barcelona, Barcelona, Spain;* [3]*University of Glasgow, Glasgow, United Kingdom; and* [4]*University of Texas Health Center at Tyler, Tyler, Texas*

Submitted 30 November 2005; accepted in final form 13 March 2006

González, José M., Ana M. Briones, Beatriz Somoza, Craig J. Daly, Elisabet Vila, Barry Starcher, John C. McGrath, M. Carmen González, and Silvia M. Arribas. Postnatal alterations in elastic fiber organization precede resistance artery narrowing in SHR. *Am J Physiol Heart Circ Physiol* 291: H804–H812, 2006. First published March 24, 2006; doi:10.1152/ajpheart.01262.2005.—Resistance artery narrowing and stiffening are key elements in the pathogenesis of essential hypertension, but their origin is not completely understood. In mesenteric resistance arteries (MRA) from spontaneously hypertensive rats (SHR), we have shown that inward remodeling is associated with abnormal elastic fiber organization, leading to smaller fenestrae in the internal elastic lamina. Our current aim is to determine whether this alteration is an early event that precedes vessel narrowing, or if elastic fiber reorganization in SHR arteries occurs because of the remodeling process itself. Using MRA from 10-day-old, 30-day-old, and 6-mo-old SHR and normotensive Wistar Kyoto rats, we investigated the time course of the development of structural and mechanical alterations (pressure myography), elastic fiber organization (confocal microscopy), and amount of elastin (radioimmunoassay for desmosine) and collagen (picrosirius red). SHR MRA had an impairment of fenestrae enlargement during the first month of life. In 30-day-old SHR, smaller fenestrae and more packed elastic fibers in the internal elastic lamina were paralleled by increased wall stiffness. Collagen and elastin levels were unaltered at this age. MRA from 6-mo-old SHR also had smaller fenestrae and a denser network of adventitial elastic fibers, accompanied by increased collagen content and vessel narrowing. At this age, elastase digestion was less effective in SHR MRA, suggesting a lower susceptibility of elastic fibers to enzymatic degradation. These data suggest that abnormal elastic fiber deposition in SHR increases resistance artery stiffness at an early age, which might participate in vessel narrowing later in life.

elastic fibers; resistance arteries; internal elastic lamina; stiffness; spontaneously hypertensive rats

SMALL ARTERY NARROWING AND stiffening are characteristic features of essential hypertension, usually termed hypertensive vascular remodeling (for reviews, Refs. 10, 37, 47). These alterations are important for the maintenance of hypertension, and they are known to contribute to the progression and cardiovascular morbidity and mortality associated with it (43). However, despite decades of study, the knowledge on the key determinants and time course development of vascular remodeling and increased vascular resistance in hypertension is still incomplete.

The extracellular matrix (ECM) is critical in the remodeling of tissues after injury or in disease (27). It is well established that elastin and collagen content is increased in hypertensive patients and in genetic or experimentally induced hypertension in animals (22, 23, 30, 42, 45). ECM might also have abnormal organization in hypertension. Thus we have previously reported alterations in the distribution of elastic fibers in the internal elastic lamina (IEL) of large (6, 11, 48) and small arteries (7) in adult spontaneously hypertensive rats (SHR), a rat model of essential hypertension. In vessels from these rats, IEL has a quite different organization from normotensive controls, having a "tighter mesh" and smaller fenestrae. We have also shown that, despite the scarce content of elastic fibers in small arteries, their spatial organization and the size of the fenestrae seem to be key for the mechanical properties of these vessels (20). The alteration in fenestrae size reported in SHR resistance arteries was also associated with vascular stiffening and narrowing (7). In the past, ECM has been perceived as a passive element that changes following a vascular insult. It is, therefore, possible that the alteration in the spatial organization of elastic fibers is a consequence of the remodeling process itself. However, there is recent evidence that shifts away from this classical view and suggests that early alterations in elastic fibers, determined genetically or by environmental factors during development, might be critical for the development of vascular diseases (9, 12). First, epidemiological studies provided a basis for the hypothesis that defective elastogenesis during fetal and early postnatal years may be an initiating event favoring the development of hypertension in adulthood (33, 34). Second, studies in cells from patients with elastin gene defects and the murine models of these diseases ($eln^{-/-}$) have show that elastin is an early determinant of arterial morphogenesis (28, 31, 51) and that elastin haploinsufficiency is associated with abnormal artery structure and mechanics and with a hypertensive phenotype (18, 46). In light of this new evidence regarding the early role of elastic fibers in arterial morphogenesis, we hypothesized that early abnormal elastic fiber deposition in vessels might participate in hypertensive vascular remodeling. To analyze this hypothesis, we have studied the time course changes in elastic fibers and collagen with vascular structure and mechanics from the first weeks of life, where elastogenesis is still active (13), until adulthood. In this study, we employed mesenteric resistance arteries (MRA) from SHR and their normotensive controls, Wistar Kyoto rats (WKY).

MATERIALS AND METHODS

Male rats, 10 ± 2 days, 30 ± 2 days, and 6 mo old, were obtained from the colonies of WKY and SHR, derived from the Charles River strains, inbred at our Animal House facilities.

Address for reprint requests and other correspondence: S. M. Arribas, Departamento de Fisiología, Facultad de Medicina, Universidad Autónoma de Madrid, C/Arzobispo Morcillo 2, 28029 Madrid, Spain (e-mail: silvia.arribas@uam.es).

The costs of publication of this article were defrayed in part by the payment of page charges. The article must therefore be hereby marked "*advertisement*" in accordance with 18 U.S.C. Section 1734 solely to indicate this fact.

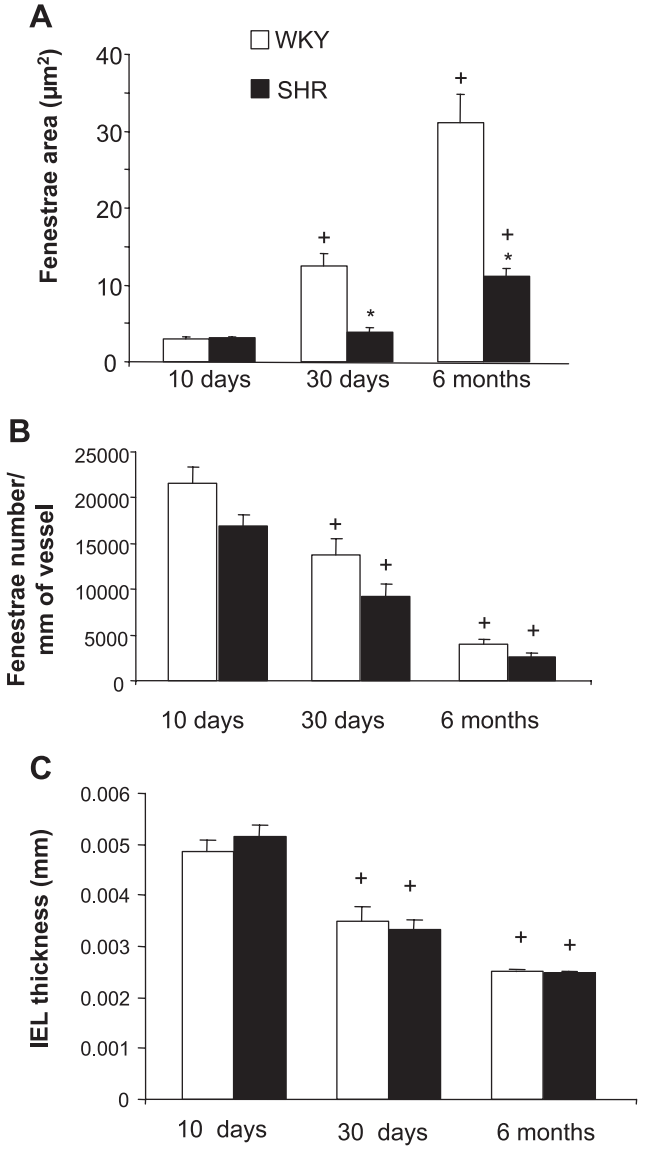

Fig. 1. Changes with age in fenestrae area and number and internal elastic lamina (IEL) thickness of mesenteric resistance arteries (MRAs) from Wistar-Kyoto rats (WKY) and spontaneously hypertensive rats (SHR). All parameters were determined in intact pressure-fixed arterial segments with confocal microscopy and image analysis software. Number of animals = 7–10 per strain and age. *$P < 0.05$ with respect to age-matched WKY; $^{+}P < 0.05$ with respect to previous age of the same strain.

Systolic blood pressure (SBP) was measured in anesthetized rats (pentobarbital sodium, 50 mg/kg ip) with a cannula inserted in the iliac artery through a pressure transducer (Statham). Thereafter, the rats were killed by bleeding, and the mesenteric bed was removed. The investigation conforms to the *Guide for the Care and Use of Laboratory Animals* published by the National Institutes of Health (NIH publication No. 85–23, revised in 1996) and with guidelines set by Spanish legislation regarding the use of experimental animals (RD 1201/2005). Eperiments were approved by the Ethics Comittee of the Faculty of Medicine.

Structural and mechanical properties of MRA. Third-order branch MRA segments were mounted on a pressure myograph (Danish Myo-Tech, model P100, J. P. Trading I/S, Aarhus, Denmark), as previously described (7). Briefly, after a 30-min equilibration period at 70 mmHg in gassed Krebs-Henseleit solution (KHS; in mM: 119 NaCl, 4.7 KCl, 2.5 $CaCl_2$, 24 $NaHCO_3$, 1.18 KH_2PO_4, 1.2 $MgSO_4$, 0.01 EDTA, and 5.5 glucose) at 37°C, a pressure-diameter curve (20–120 mmHg) was obtained in calcium-free KHS (0 Ca^{2+}; 10 mM EGTA), and internal and external diameters were measured. From these measurements, structural and mechanical parameters were calculated as previously described (4, 7, 16). Intrinsic wall stiffness was determined by the parameter β (obtained from stress-strain relationship), which is directly proportional to Young's incremental elastic modulus and a measure of intrinsic stiffness independent of geometry (16). After maximal relaxation with 0 Ca^{2+}, the artery was pressure fixed at 70 mmHg with 4% paraformaldehyde, at 37°C for 60 min for confocal microscopy study.

The effect of digestion with elastase on vascular structure, mechanics, and organization of elastic fibers was studied in MRA segments from adult rats. Briefly, after an equilibration period, as described above, MRA segments were set to 10 mmHg, allowed to equilibrate for another 15 min in gassed KHS at 37°C, and then incubated for 55 min with elastase (0.065 mg/ml in KHS, porcine pancreatic elastase; Sigma). Measurements of internal diameter were taken every 5 min. Based on these time course experiments and our laboratory's previous work (7), a group of experiments was designed to test the effect of elastase for a short (15-min) incubation period, as follows. A first pressure-diameter curve was performed in 0 Ca^{2+}. The segments were then set to 10 mmHg and equilibrated for 15 min in gassed KHS. Thereafter, they were incubated for 15 min with 0.065 mg/ml elastase, and, after 30-min washout period with 0 Ca^{2+}, a second pressure-diameter curve was obtained. All the segments were then pressure-fixed for confocal microscopy study.

Elastic fiber organization in MRA. The organization of elastic fibers in the IEL and adventitia was studied in intact pressure-fixed MRA segments with fluorescent confocal microscopy (Leica TCS SP2, Germany) based on the autofluorescent properties of elastin (excitation 488 nm/emission 500–560 nm) (52). The autofluorescence observed at this wavelength was due to elastin as it survived hot alkali digestion (7). Quantitative analysis was performed with MetaMorph Image analysis software (Universal Imaging), from confocal projec-

Table 1. *Elastin content and organization in mesenteric resistance arteries from WKY and SHR at different ages*

	10 day old		1 mo old		6 mo old	
	WKY	SHR	WKY	SHR	WKY	SHR
Desmosine content, pm/mg	Not available	Not available	1,139.5±100	1,276.6±123	1,459±101	1,354±54
IEL fluorescence intensity (average pixel)	19.0±2.9	19.4±2.4	48.9±2.4*	61.7±5.5*	47.9±7.1	52.8±4.6
IEL fluorescence intensity × relative area occupied by elastin (relative units)	8.7±1.7	9.6±1.9	29.7±21.6*	53.5±5.8*†	27.4±5.1	44.1±4.3†

Values are means ± SE; n = 5–11 rats. WKY, Wistar-Kyoto rats; SHR, spontaneously hypertensive rats; IEL, internal elastic lamina. *$P < 0.05$ compared with the previous age; †$P < 0.05$ compared with age-matched WKY.

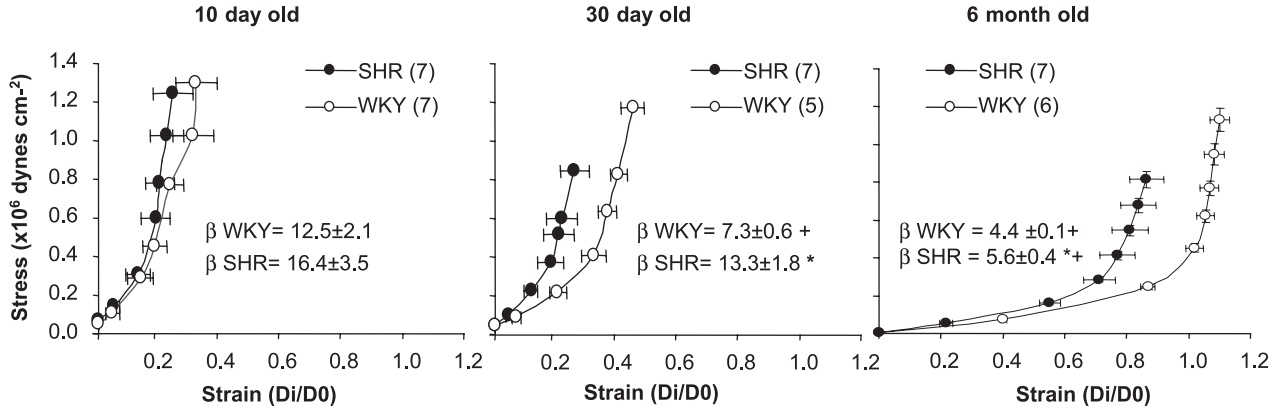

Fig. 2. Comparison of mechanical parameters in MRAs from WKY and SHR with age. Stress-strain curves with β values were obtained in pressurized MRA segments from 10- and 30-day-old and 6-mo-old WKY and SHR. No. of animals are in parentheses. $^{*}P < 0.05$ with respect to age-matched WKY; $^{+}P < 0.05$ compared with previous age point of the same strain. Di/D0, relative increase of internal diameter with pressure.

tions of serial images of the IEL and adventitia, as previously described (7). In the projections of the IEL, the following parameters were measured: size and number of fenestrae and IEL thickness. In addition, we determined how densely packed were elastic fibers in the IEL. This was estimated in the confocal projections based on fluorescence intensity values, which are directly proportional to the concentration of elastin (5), and the relative area occupied by elastic fibers, excluding fenestrae. The relative area occupied by elastic fibers was measured in binary images obtained after thresholding the confocal projections. In the binary images, elastic fibers appear in white (value

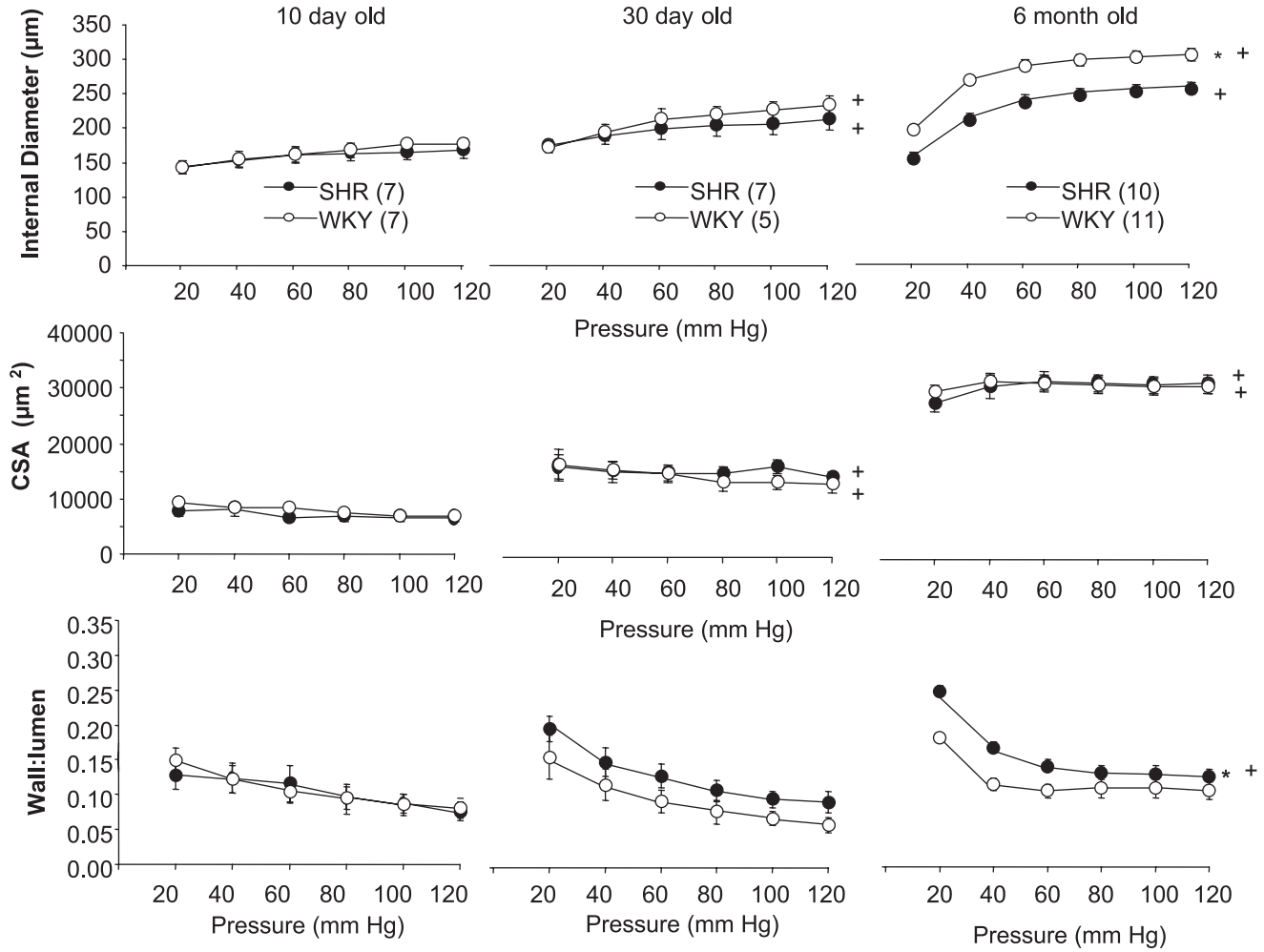

Fig. 3. Comparison of structural parameters in MRAs from WKY and SHR with age. Internal diameter, cross-sectional area (CSA), and wall-to-lumen ratio were determined in pressurized MRA segments from 10- and 30-day-old and 6-mo-old rats. No. of animals are in parentheses. $^{*}P < 0.05$ with respect to age-matched WKY; $^{+}P < 0.05$ with respect to previous age of the same strain.

1) and fenestrae in black (value 0) (7). Elastic fiber network in the adventitia was studied in projections of the external layers of the artery. These projections were thresholded, and binary images obtained. Then the relative area occupied by fibers vs. background was quantified, as described above.

Determination of elastin content. Elastin content was assessed by radioimmunoassay for desmosine, an amino acid cross link found only in elastin (17). Desmosine content was studied in third-order branches of MRA at all age points, except 10 days, at which the amount of tissue obtained was not sufficient. Briefly, paraformaldehyde-fixed vessels were hydrolyzed in 6 N HCl at 100°C for 24 h. The hydrolysates were evaporated to dryness, redissolved in 200 μl water, vortexed, microfuged, and assayed for desmosine (50) and for total protein using a ninhydrin assay (49).

Determination of collagen content. Collagen was determined with picrosirius red staining as described (26). Color images were captured with a microscope (Nikon Eclipse TE 2000-S, ×40 objective) using a digital camera (Nikon DXM 1200F). Original images of MRA ring sections were transformed to gray-scale level. Thereafter, collagen content was estimated separately in the adventitia and medial layers by subtracting the background from the intensity values obtained in the medial or adventitial areas of each ring.

Statistical analysis. Results are expressed as means ± SE, and *n* denotes the number of animals used in each experiment. The dependency of either vascular structure or mechanics on rat strain or age and intraluminal pressure was studied by a two-way ANOVA, followed by a Bonferroni correction for multiple comparisons. For specific two means comparisons, Student's *t*-test (paired or unpaired) was used.

RESULTS

Time course development of vascular remodeling, elastic fiber, and collagen alterations in MRA from SHR and WKY rats. At the age of 10 days, SHR showed similar SBP, compared with age-matched WKY rats (SHR = 43.2 ± 3.4 mmHg, $n = 9$; WKY = 36.4 ± 2.0 mmHg, $n = 8$). At this age, the amount of MRA obtained was not sufficient for quantification of elastin based on desmosine determination. However, IEL structure could be determined with confocal microscopy. This approach showed that elastic fibers were similarly packed in both strains. Thus fenestrae size and number, IEL thickness, and fluorescence intensity values were similar in WKY and SHR (Fig. 1, Table 1). Stress-strain relationship, and β value (an indicator of intrinsic wall stiffness independent of geometry) were similar in SHR and WKY (Fig. 2). Similarly, no structural differences in the wall of MRA were found at this age. Thus internal diameter, cross-sectional area (CSA), and wall-to-lumen ratio (Fig. 3) were also similar between strains.

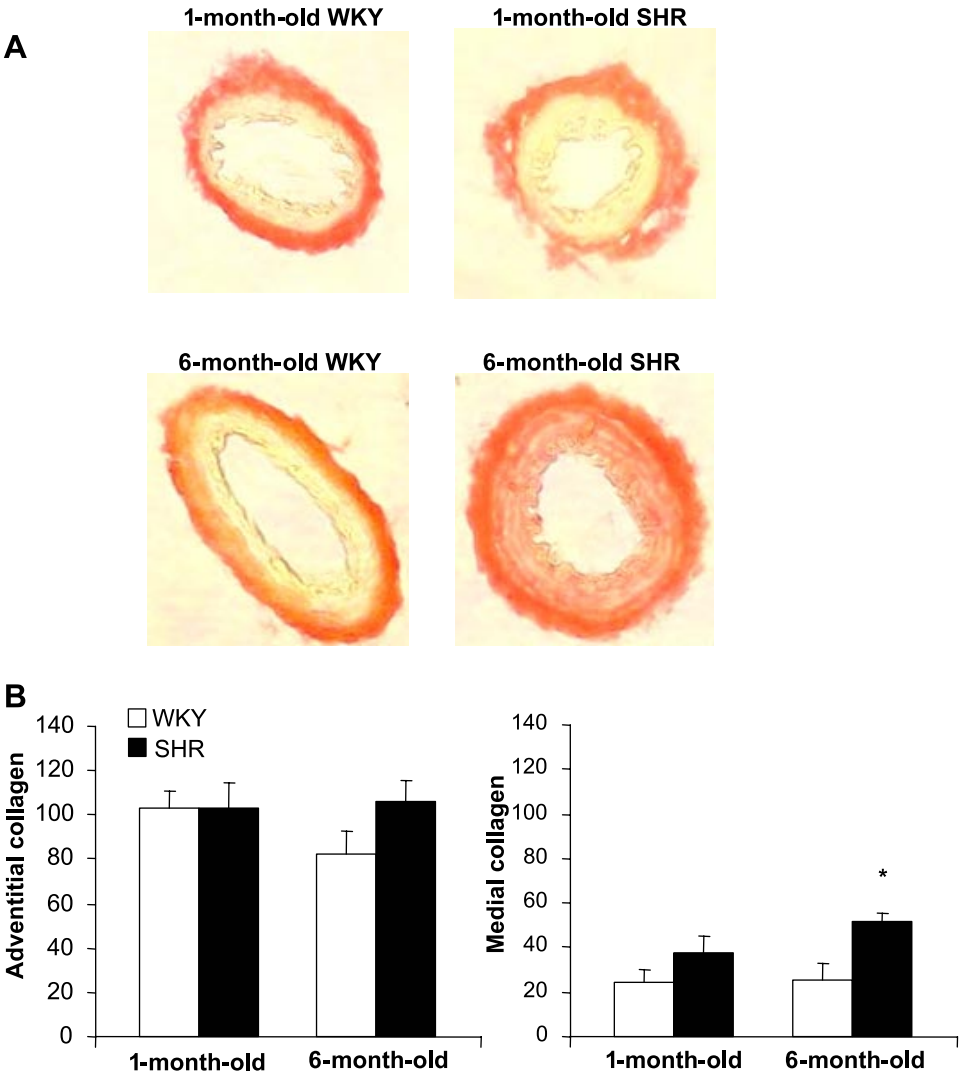

Fig. 4. Comparison of collagen content in MRAs from WKY and SHR with age. *A*: representative images of the distribution of collagen in the media and adventitia in MRA rings from 1- and 6-mo-old WKY and SHR stained with picrosirius red. *B*: quantification of adventitial and medial collagen content by image analysis software. *$P < 0.05$ with respect to age-matched WKY.

At the age of 30 days, SBP was still similar between strains (SHR = 99 ± 4.0 mmHg, n = 14; WKY = 89 ± 4.7 mmHg, n = 15). From the age of 10–30 days, MRA from normotensive WKY had a significant enlargement of fenestrae area. However, in SHR vessels, fenestrae area did not increase during this 3-wk period. As a result, in 30-day-old SHR, the IEL was more "densely packed," with an increased relative area occupied by elastic fibers and, accordingly, a significantly smaller fenestrae size and a tendency toward larger fluorescence intensity values (P = 0.061) compared with age-matched WKY (Fig. 1, Table 1). In both strains, there was a parallel decrease in fenestrae number (Fig. 1*B*) and IEL thickness (Fig. 1*C*) with age: at the age of 30 days, there was no difference between WKY and SHR in these parameters or in total elastin (Table 1) or collagen (Fig. 4) contents. From the 10th to the 30th day of life, β values decreased significantly in MRA from WKY, but did not change in arteries from SHR. Consequently, there was a significantly higher β value and thus an increased intrinsic stiffness, in MRA from 30-day-old SHR compared with age-matched WKY (Fig. 2). During this 3-wk period, both strains experienced an age-dependent increase in internal diameter and CSA, but not in wall-to-lumen ratio. By the age of 30 days, all structural parameters were still similar between WKY and SHR (Fig. 3).

At the age of 6 mo, SBP was significantly elevated in SHR (SHR = 183.4 ± 10.4 mmHg, n = 10; WKY = 127.2 ± 10 mmHg, n = 8). From the 1st to the 6th mo of life, there was a further increase in fenestrae area and a decrease in fenestrae number in MRA from both strains (Fig. 1, *A* and *B*) with a negative correlation between both parameters in WKY (R =

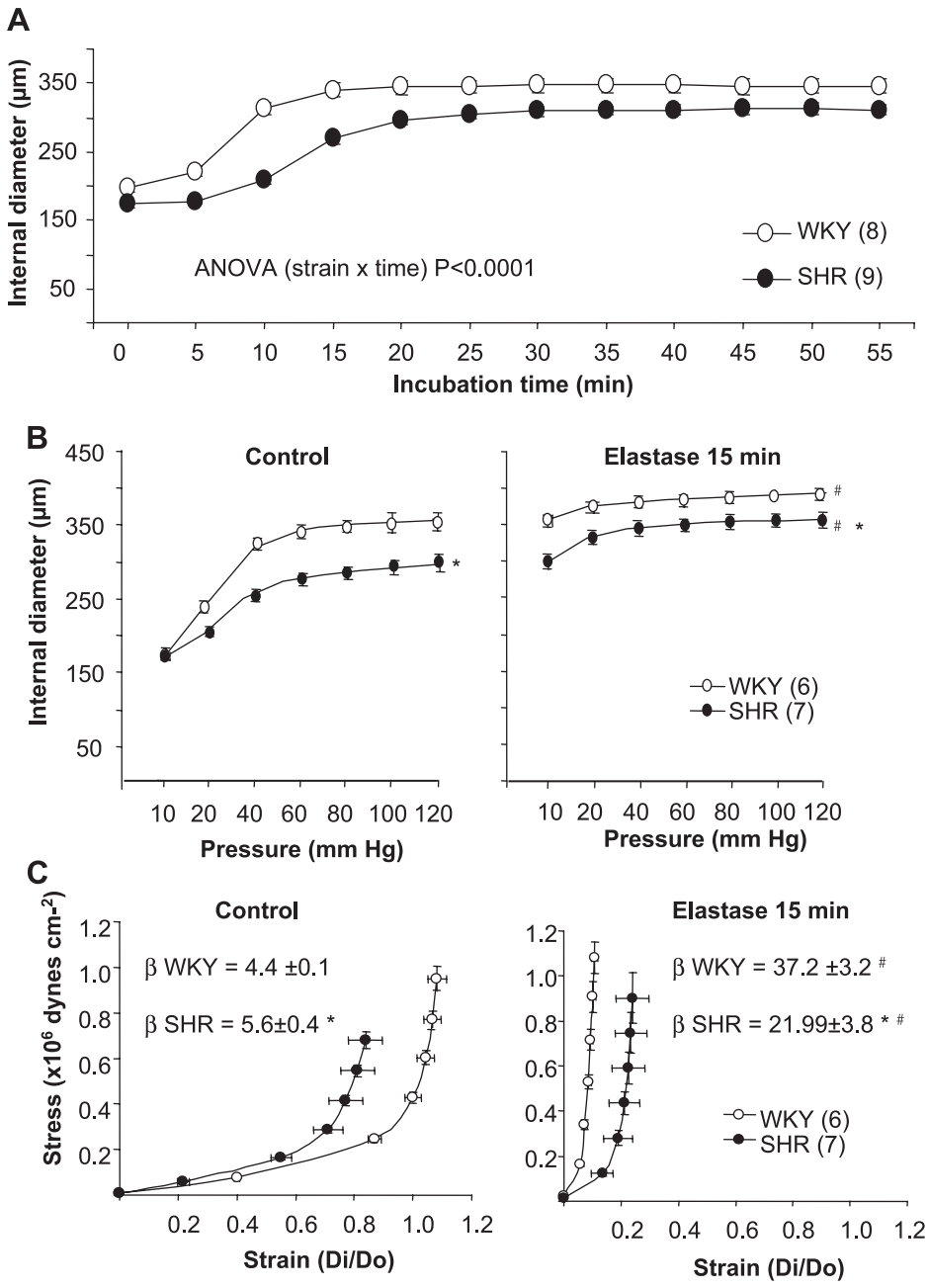

Fig. 5. Effect of elastase (0.065 mg/ml) on vascular structure and mechanics of MRAs from 6-mo-old WKY and SHR. *A*: effect of incubation time on internal diameter of MRA pressurized at 10 mmHg. *B*: effect of 15-min elastase incubation on internal diameter-pressure curves. *C*: effect of 15-min elastase incubation on stress-strain curves and β values. No. of animals are in parentheses. *P < 0.05 compared with WKY; #P < 0.05 compared with control segments (before elastase incubation; paired experiments) of the same strain.

0.86) and in SHR ($R = 0.86$). The percent enlargement of fenestrae during this 5-mo period was similar in both strains (WKY = 60%, SHR = 65%). Thus fenestrae size remained smaller in MRA from 6-mo-old SHR compared with age-matched WKY (Fig. 1*A*). IEL thickness further decreased during this 5-mo period in both WKY and SHR with no significant difference between strains (Fig. 1*C*). Total elastin content was not modified from *month 1* to *month 6* of life in either WKY or SHR, and it was similar between strains (Table 1). Collagen content increased during this 5-mo period in SHR, but not in WKY MRA, resulting in significantly larger content in vessels from adult SHR (Fig. 4). From *month 1* to *month 6* of life, β values further decreased in both strains and remained significantly higher in SHR (Fig. 2). During this 5-mo period, arteries from both strains experienced an age-dependent increase in all structural parameters. At the age of 6 mo, SHR vessels showed the characteristic features of eutrophic inward remodeling, i.e., a reduced internal diameter, unchanged CSA, and an increased wall-to-lumen ratio (Fig. 3).

Elastin degradation experiments in MRA from adult WKY and SHR. In MRA from 6-mo-old rats, elastase incubation for 55 min significantly increased internal diameter in both strains. The increase at each incubation time was greater in WKY than in SHR for the first 20 min; after that the curves were parallel (Fig. 5*A*). Short (15 min) incubation with elastase induced an increase in internal diameter-pressure curves in both strains. In SHR, internal diameter remained significantly smaller compared with WKY (Fig. 5*B*). Incubation for 15 min with elastase induced a marked shift to the left of the stress-strain relationship and a significant increase of β in both strains. This effect was less marked in SHR arteries compared with WKY MRA (Fig. 5*C*). Elastin digestion for 15 min significantly enlarged fenestrae size in the IEL of both strains. After digestion, SHR fenestrae remained significantly smaller compared with WKY (Fig. 6). In the outer part of MRA, elastic fibers were distributed in a network, which was more densely organized in SHR vessels (Fig. 7, *A* and *B*). After 15-min incubation with elastase, elastic fibers were still present in SHR arteries, while they were completely eliminated in WKY MRA (Fig. 7*C*).

DISCUSSION

In our previous study (7) in resistance arteries from SHR, we observed an association between abnormal IEL organization due to smaller fenestrae and inward remodeling. We have now investigated the time course development of these alterations to

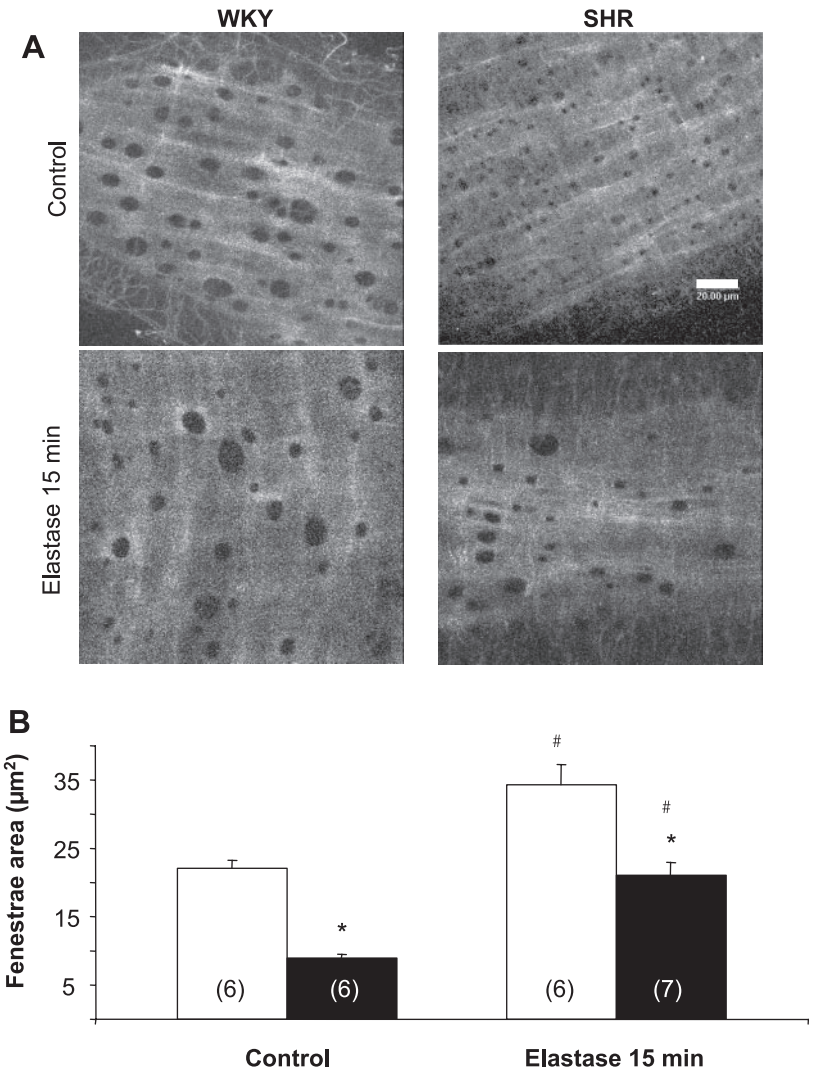

Fig. 6. Effect of 15-min elastase (0.065 mg/ml) incubation on fenestrae size in the IEL of MRAs from 6-mo-old WKY and SHR. Representative images (*A*) and quantification (*B*) of fenestrae area in IEL projections from WKY (open bars) and SHR (filled bars) MRA are shown before (control) and after incubation with elastase. No. of animals are in parentheses. Projections were obtained from serial optical sections captured with a fluorescence confocal microscope (excitation 488 nm, emission 500–560 nm; ×63 oil immersion objective; bar = 20 μm). $*P < 0.05$ with respect to WKY; $\#P < 0.05$ compared with control segments (without elastase) of the same strain.

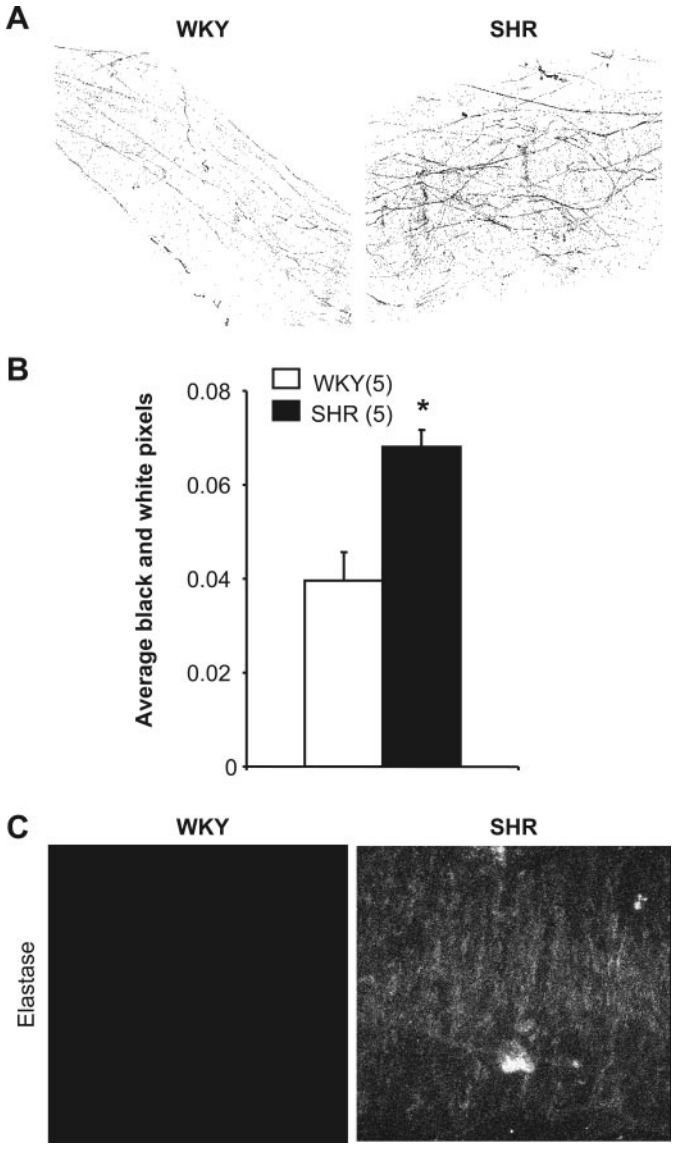

Fig. 7. Effect of 15-min elastase (0.065 mg/ml) incubation on the organization of adventitial elastic fibers in MRAs from WKY and SHR. *A*: binary images obtained from confocal projections of the adventitia of MRA segments from a WKY and a SHR. *B*: quantification of elastic fibers in the adventitia. *C*: confocal projections of the adventitia of MRA segments from a WKY and a SHR after elastase incubation. No. of animals are in parentheses. Projections were obtained from serial optical sections captured with a fluorescence confocal microscope (excitation 488 nm, emission 500–560 nm; ×63 oil immersion objective). *$P < 0.05$ with respect to WKY.

determine whether the reduction in fenestrae size occurs because of vascular remodeling or precedes it. Our data suggest this second possibility and that, in SHR, changes in elastic fiber deposition during development and before the establishment of hypertension lead to abnormal, more densely packed IEL. This defect increases vessel stiffness at an early age, which might participate in the development of hypertensive inward remodeling in adulthood.

In the IEL, fenestrae enlarge along with artery development by fusion of neighboring fenestrae (52). This was also demonstrated in our study by the negative correlation between fenestrae number and area in both strains during arterial growth. However, this normal enlargement of fenestrae was impaired in SHR vessels during the first weeks of postnatal life. Thus the time course study of collagen and elastic fibers showed that the first visible alteration of these ECM proteins in SHR MRA was a reduction of fenestrae size, leading to a more compact IEL by the first month of life. The present data also demonstrate that this alteration was paralleled by increased intrinsic wall stiffness. This was shown by the fact that the gradual reduction of wall stiffness with age (decrease in β values) that occurs in WKY along with fenestrae growth was hampered in SHR vessels between the 10th and the 30th day, in parallel with the deficient fenestrae enlargement. However, the structural alterations (reduced vessel diameter, increased wall CSA, and wall-to-lumen ratio) develop later in life and could be related to the IEL alteration and concomitant increased MRA stiffness. In fact, increased vessel stiffness has been proposed as one of the possible mechanisms implicated in small artery narrowing in hypertension (10).

Increased vessel stiffness in hypertension has been generally attributed to increased collagen content. In fact, it is well established that hypertension stimulates collagen production (8, 19, 21–23, 30, 42, 45). The present data also show that, in resistance arteries, collagen content was higher in SHR, but only in adult rats. Quantitative differences in collagen were not yet present by the first month of life, before high blood pressure development. Total elastin content was also similar between strains in young and in adult rats. Therefore, the increased stiffness observed in resistance arteries from SHR, before hypertension development, is likely to be related to qualitative alterations of elastic fiber distribution, leading to a more compact IEL. This is in agreement with our recent finding that, in small cerebral and mesenteric arteries from normotensive rats, intrinsic wall stiffness correlates better with the size of the fenestrae in the IEL than with total collagen or elastin content (20). In addition to a more compact IEL, SHR vessels also showed a denser elastic fiber distribution in the adventitial side of the artery. This alteration might also contribute to the elevated intrinsic vascular stiffness in SHR.

Reduced fenestra enlargement in SHR might be related to the observed differences in elastic fiber organization, which might be less susceptible to degradation. We tested this hypothesis with time course experiments with elastase. This enzyme has been shown to induce degradation of elastic fibers in blood vessels (7, 32). In our previous study (7), we demonstrated that prolonged incubation periods (over 50 min) with elastase eliminated elastic fiber network in the adventitia and merged neighboring fenestrae, disrupting IEL organization both in WKY and SHR. The present time course experiments showed that, during the first 20 min, elastase increased vessel diameter more rapidly in WKY vessels. We, therefore, used short incubation periods with elastase and demonstrate that elastic fibers from SHR show a lower susceptibility to degradation. This was supported by the fact that isolated fibers were still present in the adventitia of SHR, whereas adventitial elastin disappeared completely from WKY vessels. This is likely to be related to the denser organization of fibers in SHR, making them less prone to enzymatic digestion. The presence of more elastin left in SHR after short time digestion was also confirmed by the vascular mechanical behavior. Thus, while SHR MRAs were stiffer than WKY before elastin degradation, after digestion, SHR vessels became less stiff compared with

WKY. We, therefore, suggest that the more compact organization of elastic fibers in the vascular wall of SHR makes them less susceptible to degradation than those from WKY.

The differences in susceptibility to digestion by elastase, leading to a more compact IEL and denser adventitial elastic fiber network, might be explained by a higher elastin content in SHR vessels. In favor of this hypothesis is the fact that, in SHR and the stroke-prone strain, augmented elastin content has been reported in large arteries before full establishment of hypertension (3, 15) and even in fetal and neonatal rats (24). We did not find significant differences in elastic fiber content in resistance arteries between strains, but we cannot discard the existence of small changes below the level of detection with current methodology.

A second possibility is that the lower susceptibility to degradation of SHR elastic fibers is related to differences in amino acid composition. Enzymatic degradation of elastin is influenced by the amino acid residues (35), and differences have been reported between WKY and SHR aortas, with the latter showing a higher proportion of polar amino acids (14, 15, 25, 40).

Elastic fiber synthesis is complex because of its multiple components, tightly regulated developmental pattern of deposition, and multistep hierarchical assembly. With the exception of several reports on elastin content, elastic fiber biology is largely unknown in WKY and SHR vessels, which makes it difficult to speculate on the possible mechanisms participating in the development of a more compact elastic fiber distribution in SHR arteries. The fact that this defect is observed in both conduit (6, 11, 48) and resistance arteries (7) from SHR and stroke-prone SHR, and, so far, it has not been found in nongenetic models of hypertension (8), suggests that it might be related to a genetic alteration in a component of the elastic fiber and/or to a protein involved in its assembly or maturation. In this sense, there is evidence linking genetic alterations in several components of elastic fibers, with vascular mechanical abnormalities and hypertension (for review, see Ref. 2). Among others, mutations in tropoelastin (18, 46), fibulin-5 (53), and fibrillin-1 genes (36) have been linked to large-artery stiffness, sometimes linked with hypertensive phenotype or elevations in pulse pressure. In addition, we have to consider the possibility that alterations in the metabolism of factors that modulate elastic fiber formation could participate in the defect observed in SHR arteries. Among others, abnormal levels of copper (29), magnesium (41), vitamin D (38), or iron (1) have been linked to cardiovascular diseases.

The present data also demonstrate that the defect in fenestrae enlargement takes place before the development of hypertension in SHR, which occurs in this strain by the third month of life (39). This alteration seems to be independent of the level of blood pressure, as suggested by the similar percentage of fenestrae enlargement in both strains from the first to the sixth month of life and by our recent findings showing no changes in IEL structure in an experimental model of hypertension induced by chronic administration of ouabain (8). This defect seems to be generalized in the vasculature of SHR. We have not studied whether it follows the same developmental pattern and whether it modifies vascular mechanical properties of large vessels. If that were the case, an early compromise in large artery compliance might participate in the development of hypertension in this rat model.

Future perspectives. Since elastic fibers are only actively synthesized during embryonic development and early postnatal years (13, 44) and they are critical for vascular mechanical properties, it has been proposed that defective elastogenesis could be an initiating event in the pathogenesis of essential hypertension (33, 34). So far, this link is circumstantial and derived from *1*) epidemiological studies relating birth size and hypertension development, and *2*) abnormal vascular mechanics and hypertension in human diseases related to mutations of elastic fiber molecules. However, abnormalities in elastic fibers have not been thoroughly studied in arteries from patients with essential hypertension. The present study provides evidence that, in SHR, a rat model of the disease, an early abnormality in elastic fibers is associated with increased vascular stiffness. Obviously, the next step would be to determine whether this abnormality also exists in arteries from essential hypertensive patients. If so, polymorphisms of genes related to molecules linked to elastic fiber synthesis or degradation, as well as the effect of current antihypertensive treatment, could be investigated (12, 18). In addition, it would also be of great value to determine, in animal models, the effect of dietary factors that influence elastogenesis on elastic fiber organization and vascular mechanical properties.

ACKNOWLEDGMENTS

We are grateful to Diego Megías for assistance with confocal microscopy, Dr. M. Carmen Fernández-Criado for the maintenance of the rat colonies, and Dr. Jesus Giraldo for help with the statistical analysis.

GRANTS

This study was supported by the European Union (QLG-CT-1999–00084); SAF 2000–1877-CE; Ministerio de Ciencia y Tecnología (BFU 2004–04148), Acciones Integradas, and Comunidad Autónoma de Madrid (GRSAL 0093–2004), Spain.

REFERENCES

1. **Aessopos A, Farmakis D, and Loukopoulos D.** Elastic tissue abnormalities in inherited haemolytic syndromes. *Eur J Clin Invest* 32: 640–642, 2002.
2. **Arribas S, Hinek A, and González MC.** Elastic fibres and vascular structure in hypertension. *Pharmacol Ther.* In press.
3. **Baccarani Contri M, Taparelli F, Miselli M, Bacchelli B, and Biagini G.** Histomorphometric, biochemical and ultrastructural changes in the aorta of salt-loaded stroke-prone spontaneously hypertensive rats fed a Japanese-style diet. *Nutr Metab Cardiovasc Dis* 13: 37–45, 2003.
4. **Baumbach GL and Heistad DD.** Remodeling of cerebral arterioles in chronic hypertension. *Hypertension* 13: 968–972, 1989.
5. **Blomfield J and Farrar JF.** The fluorescent properties of maturing arterial elastin. *Cardiovasc Res* 3: 161–170, 1969.
6. **Boumaza S, Arribas SM, Osborne-Pellegrin M, McGrath JC, Laurent S, Lacolley P, and Challande P.** Fenestrations of the carotid internal elastic lamina and structural adaptation in stroke-prone spontaneously hypertensive rats. *Hypertension* 37: 1101–1107, 2001.
7. **Briones AM, Gonzalez JM, Somoza B, Giraldo J, Daly CJ, Vila E, Gonzalez MC, McGrath JC, and Arribas SM.** Role of elastin in spontaneously hypertensive rat small mesenteric artery remodelling. *J Physiol* 552: 185–195, 2003.
8. **Briones AM, Xavier FE, Arribas SM, Gonzalez MC, Rossoni LV, Alonso MJ, and Salaices M.** Alterations in structure and mechanics of resistance arteries from ouabain induced hypertensive rats. *Am J Physiol Heart Circ Physiol*. In press.
9. **Brooke BS, Bayes-Genis A, and Li DY.** New insights into elastin and vascular disease. *Trends Cardiovasc Med* 13: 176–181, 2003.
10. **Bund SJ and Lee RM.** Arterial structural changes in hypertension: a consideration of methodology, terminology and functional consequence. *J Vasc Res* 40: 547–557, 2003.

11. **Cohuet G, Challande P, Osborne-Pellegrin M, Arribas SM, Dominiczak A, Louis H, Laurent S, and Lacolley P.** Mechanical strength of the isolated carotid artery in SHR. *Hypertension* 38: 1167–1171, 2001.
12. **D'Armiento J.** Decreased elastin in vessel walls puts the pressure on. *J Clin Invest* 112: 1308–1310, 2003.
13. **Davis EC.** Elastic lamina growth in the developing mouse aorta. *J Histochem Cytochem* 43: 1115–1123, 1995.
14. **Deyl Z, Horakova M, and Macek K.** Changes in elastin composition in aorta of spontaneously hypertensive rats (SHR). *Biochem Biophys Res Commun* 129: 179–186, 1985.
15. **Deyl Z, Jelinek J, Macek K, Chaldakov G, and Vankov VN.** Collagen and elastin synthesis in the aorta of spontaneously hypertensive rats. *Blood Vessels* 24: 313–320, 1987.
16. **Dobrin PB.** Mechanical properties of arterises. *Physiol Rev* 58: 397–460, 1978.
17. **Eyre DR, Paz MA, and Gallop PM.** Cross-linking in collagen and elastin. *Annu Rev Biochem* 53: 717–748, 1984.
18. **Faury G, Pezet M, Knutsen RH, Boyle WA, Heximer SP, McLean SE, Minkes RK, Blumer KJ, Kovacs A, Kelly DP, Li DY, Starcher B, and Mecham RP.** Developmental adaptation of the mouse cardiovascular system to elastin haploinsufficiency. *J Clin Invest* 112: 1419–1428, 2003.
19. **Fridez P, Zulliger M, Bobard F, Montorzi G, Miyazaki H, Hayashi K, and Stergiopulos N.** Geometrical, functional, and histomorphometric adaptation of rat carotid artery in induced hypertension. *J Biomech* 36: 671–680, 2003.
20. **Gonzalez JM, Briones AM, Starcher B, Conde MV, Somoza B, Daly C, Vila E, McGrath I, Gonzalez MC, and Arribas SM.** Influence of elastin on rat small artery mechanical properties. *Exp Physiol* 90: 463–468, 2005.
21. **Hadjiisky P, Peyri N, and Grosgogeat Y.** Tunica media changes in the spontaneously hypertensive rat (SHR). *Atherosclerosis* 65: 125–137, 1987.
22. **Intengan HD, Deng LY, Li JS, and Schiffrin EL.** Mechanics and composition of human subcutaneous resistance arteries in essential hypertension. *Hypertension* 33: 569–574, 1999.
23. **Intengan HD, Thibault G, Li JS, and Schiffrin EL.** Resistance artery mechanics, structure, and extracellular components in spontaneously hypertensive rats: effects of angiotensin receptor antagonism and converting enzyme inhibition. *Circulation* 100: 2267–2275, 1999.
24. **Iredale RB, Eccleston-Joyner CA, Rucker RB, and Gray SD.** Ontogenic development of the elastic component of the aortic wall in spontaneously hypertensive rats. *Clin Exp Hypertens* 11: 173–187, 1989.
25. **Ito H, Yamamoto K, and Okamoto K.** On elastin in aorta of SHRSP (2). *Jpn Heart J* 19: 568–569, 1978.
26. **Izzard AS, Graham D, Burnham MP, Heerkens EH, Dominiczak AF, and Heagerty AM.** Myogenic and structural properties of cerebral arteries from the stroke-prone spontaneously hypertensive rat. *Am J Physiol Heart Circ Physiol* 285: H1489–H1494, 2003.
27. **Jacob MP, Badier-Commander C, Fontaine V, Benazzoug Y, Feldman L, and Michel JB.** Extracellular matrix remodeling in the vascular wall. *Pathol Biol (Paris)* 49: 326–332, 2001.
28. **Karnik SK, Brooke BS, Bayes-Genis A, Sorensen L, Wythe JD, Schwartz RS, Keating MT, and Li DY.** A critical role for elastin signaling in vascular morphogenesis and disease. *Development* 130: 411–423, 2003.
29. **Klevay LM.** Cardiovascular disease from copper deficiency–a history. *J Nutr* 130: 489S–492S, 2000.
30. **Laviades C, Varo N, Fernandez J, Mayor G, Gil MJ, Monreal I, and Diez J.** Abnormalities of the extracellular degradation of collagen type I in essential hypertension. *Circulation* 98: 535–540, 1998.
31. **Li DY, Brooke B, Davis EC, Mecham RP, Sorensen LK, Boak BB, Eichwald E, and Keating MT.** Elastin is an essential determinant of arterial morphogenesis. *Nature* 393: 276–280, 1998.
32. **Martin BJ, Stehbens WE, Davis PF, and Ryan PA.** Scanning electron microscopic study of hemodynamically induced tears in the internal elastic lamina of rabbit arteries. *Pathology* 21: 207–212, 1989.
33. **Martyn CN and Greenwald SE.** A hypothesis about a mechanism for the programming of blood pressure and vascular disease in early life. *Clin Exp Pharmacol Physiol* 28: 948–951, 2001.
34. **Martyn CN and Greenwald SE.** Impaired synthesis of elastin in walls of aorta and large conduit arteries during early development as an initiating event in pathogenesis of systemic hypertension. *Lancet* 350: 953–955, 1997.
35. **Mecham RP, Broekelmann TJ, Fliszar CJ, Shapiro SD, Welgus HG, and Senior RM.** Elastin degradation by matrix metalloproteinases. Cleavage site specificity and mechanisms of elastolysis. *J Biol Chem* 272: 18071–18076, 1997.
36. **Medley TL, Cole TJ, Gatzka CD, Wang WY, Dart AM, and Kingwell BA.** Fibrillin-1 genotype is associated with aortic stiffness and disease severity in patients with coronary artery disease. *Circulation* 105: 810–815, 2002.
37. **Mulvany MJ.** Small artery remodeling in hypertension. *Curr Hypertens Rep* 4: 49–55, 2002.
38. **Norman P, Moss I, Sian M, Gosling M, and Powell J.** Maternal and postnatal vitamin D ingestion influences rat aortic structure, function and elastin content. *Cardiovasc Res* 55: 369–374, 2002.
39. **Okamoto K and Aoki K.** Development of a strain of spontaneously hypertensive rats. *Jpn Circ J* 27: 282–293, 1963.
40. **Prodanov KG, Deyl Z, Jelinek J, and Macek K.** Changes in the blood vessel wall elastin of spontaneously hypertensive (SHR) rats. *Physiol Bohemoslov* 36: 481–485, 1987.
41. **Rayssiguier Y, Mbega JD, Durlach V, Gueux E, Durlach J, Giry J, Dalle M, Mazur A, Laurant P, and Berthelot A.** Magnesium and blood pressure. I. Animal studies. *Magnes Res* 5: 139–146, 1992.
42. **Rizzoni D, Muiesan ML, Porteri E, Salvetti M, Castellano M, Bettoni G, Tiberio G, Giulini SM, Monteduro C, Garavelli G, and Agabiti-Rosei E.** Relations between cardiac and vascular structure in patients with primary and secondary hypertension. *J Am Coll Cardiol* 32: 985–992, 1998.
43. **Rizzoni D, Porteri E, Boari GE, De Ciuceis C, Sleiman I, Muiesan ML, Castellano M, Miclini M, and Agabiti-Rosei E.** Prognostic significance of small-artery structure in hypertension. *Circulation* 108: 2230–2235, 2003.
44. **Rosenbloom J, Abrams WR, and Mecham R.** Extracellular matrix 4: the elastic fiber. *FASEB J* 7: 1208–1218, 1993.
45. **Rossi GP, Cavallin M, Belloni AS, Mazzocchi G, Nussdorfer GG, Pessina AC, and Sartore S.** Aortic smooth muscle cell phenotypic modulation and fibrillar collagen deposition in angiotensin II-dependent hypertension. *Cardiovasc Res* 55: 178–189, 2002.
46. **Salaymeh KJ and Banerjee A.** Evaluation of arterial stiffness in children with Williams syndrome: Does it play a role in evolving hypertension? *Am Heart J* 142: 549–555, 2001.
47. **Schiffrin EL.** Remodeling of resistance arteries in essential hypertension and effects of antihypertensive treatment. *Am J Hypertens* 17: 1192–1200, 2004.
48. **Somoza B, Abderrahim F, Gonzalez JM, Conde MV, Arribas SM, Starcher B, Regadera J, Fernandez-Alfonso MS, Diaz-Gil JJ, and Gonzalez MC.** Short-term treatment of spontaneously hypertensive rats with liver growth factor reduces carotid artery fibrosis, improves vascular function, and lowers blood pressure. *Cardiovasc Res* 69: 764–771, 2006.
49. **Starcher B.** A ninhydrin-based assay to quantitate the total protein content of tissue samples. *Anal Biochem* 292: 125–129, 2001.
50. **Starcher B and Conrad M.** A role for neutrophil elastase in the progression of solar elastosis. *Connect Tissue Res* 31: 133–140, 1995.
51. **Urban Z, Riazi S, Seidl TL, Katahira J, Smoot LB, Chitayat D, Boyd CD, and Hinek A.** Connection between elastin haploinsufficiency and increased cell proliferation in patients with supravalvular aortic stenosis and Williams-Beuren syndrome. *Am J Hum Genet* 71: 30–44, 2002.
52. **Wong LC and Langille BL.** Developmental remodeling of the internal elastic lamina of rabbit arteries: effect of blood flow. *Circ Res* 78: 799–805, 1996.
53. **Yanagisawa H, Davis EC, Starcher BC, Ouchi T, Yanagisawa M, Richardson JA, and Olson EN.** Fibulin-5 is an elastin-binding protein essential for elastic fibre development in vivo. *Nature* 415: 168–171, 2002.